the plant journal

SEB SOCIETY FOR EXPERIMENTAL BIOLOGY

The Plant Journal (2026) **125,** e70664 doi: 10.1111/tpj.70664

Synteny-based comparative pan-genome reveals a male-specific *FT* gene underlying flowering time dimorphism in kiwifruit

Le Xu[1,†], Tonghao Miao[1,†], Zhongru Cui[1,†], Erika Varkonyi-Gasic[2], Anmeng Zhang[1], Lihuan Wang[1], Bingjie Li[1,3], Andrew C Allan[2,4], Yongsheng Liu[1,*], Songhu Wang[1,*], Xueren Yin[1,5,*] and Junyang Yue[1,3,*]

[1]*Anhui Province Key Laboratory of Horticultural Crop Quality Biology, School of Horticulture, Anhui Agricultural University, Hefei 230036, China,*

[2]*Plant & Food Research, Mt Albert, Auckland 1142, New Zealand,*

[3]*Research Center for Biological Breeding, Advanced Academy, Anhui Agricultural University, Hefei 230036, China,*

[4]*School of Biological Sciences, University of Auckland, Private Bag, 92019 Auckland, New Zealand, and*

[5]*One Belt and One Road International Joint Research Center of Horticultural Products Quality and Post-Harvest Biotechnology in Anhui Province, Hefei 230036, China*

Received 24 July 2025; revised 8 October 2025; accepted 2 December 2025.
*For correspondence (e-mail liuyongsheng1122@ahau.edu.cn and wangsonghu@ahau.edu.cn and fruitquality@ahau.edu.cn and yuejy@ahau.edu.cn).
†These authors contributed equally to this work.

SUMMARY

***Actinidia* spp. (kiwifruit) are functionally dioecious with separate male and female individuals that exhibit a subtle difference in flowering time. However, this sexually dimorphic trait, along with its evolutionary history and the role of sexually antagonistic selection, remains to be fully understood. To investigate the underlying causes of this dimorphism at the genus level, we conducted a comparative pan-genome analysis of two representative kiwifruit species, *Actinidia chinensis* and *Actinidia eriantha*, using 10 chromosome-scale genome assemblies from six distinct male and female genotypes. The construction of the pan-genome revealed a total of 52 774 non-redundant pan-gene orthogroups comprising 42 370 gene clusters and 10 404 unassigned genes. Building on this, the comparative analysis further identified 657 syntenic gene sets belonging to 595 pan-gene orthogroups that exhibit significant inter-sexual divergence. It is plausible that they are drivers of the antagonistic selection responsible for conserved sexually dimorphic traits across the extant kiwifruit species. One of these genes is *Y-linked FT* (*YFT*), a male-specific variant of *FLOWERING LOCUS T* that originated following the recent whole-genome duplication event. We demonstrate that *A. eriantha YFT* is able to promote flowering, suggesting that it may contribute to the sexual dimorphism in kiwifruit flowering time. Notably, *YFT* is located in the sex-determining region (SDR), with linkage to the sex-determining genes, facilitating its spread in natural populations and SDR's expansion on the Y chromosome. For ease of use and analysis, the entire comparative pan-genome workflow was integrated into a custom Perl script, SynPanScan. This approach helps decipher the genetic basis of flowering sexual dimorphism in kiwifruit and establishes a synteny-based comparative pan-genomic framework for investigating the heritable architecture of natural phenotypic variation.**

Keywords: kiwifruit, comparative pan-genome, sex chromosome evolution, sexual dimorphism, flowering time, *FT* gene family.

INTRODUCTION

Sexual dimorphism is a remarkable feature of adaptive evolution in species with separate sexes (Williams & Carroll, 2009). Divergent reproductive strategies between males and females can result in strikingly different morphological phenotypes, such as color, shape, weight, size, and behavioral traits (Barrett & Hough, 2013; Pennell et al., 2016). Genetically, functional genes in the two sexes will be differentially selected and fixed to reach their respective fitness optima for shared traits. However, responses to these opposing selective pressures are constrained by a common genetic basis, leading to sexual antagonism, in which distinct alleles for a given gene tend to be concurrently created within natural populations

(Kaufmann et al., 2023). Accordingly, sexually antagonistic (SA) selection arises when an allele is beneficial to one sex but detrimental to the other.

SA selection is thought to be inescapable, and even pervasive in both animal and plant populations. Theoretically, SA selection on ordinary autosomes can occur only if its benefits to one sex are greater than its detriments to the other, which would diminish the ability to fix beneficial mutations through natural selection (Pennell et al., 2016). Alternatively, to prevent the production of unfavorable phenotypes in opposite sexes, SA polymorphisms often accumulate on sex chromosomes, where homologous recombination is partially or globally inhibited (Jordan & Charlesworth, 2012). In this case, a male-beneficial and/or female-detrimental allele located on the Y chromosome can be stably inherited and maintained during the life history of males, and vice versa. Furthermore, based on the prevailing theory of sex chromosome evolution, once SA polymorphisms have become fixed around the sex-determining genes, they can in turn drive the positive selection for reduced chromosomal recombination between SA loci and sex-determining loci (Ming et al., 2011). Therefore, SA selection not only has significant effects on the acquisition of sexual dimorphism, but also plays important roles in the evolutionary dynamics of sex chromosome, especially at the early stages of sex chromosome differentiation.

Actinidia spp., commonly known as kiwifruit, are native to China and consist of approximately 54 species with ploidy levels ranging from diploid to octoploid (Li et al., 2007). Despite the high genetic diversity, all species in this genus are functionally dioecious with a unisexual floral morphology and an XX/XY sex determination system. It has been known that sex determination of kiwifruit is controlled by two sex-determining genes, *Shy Girl* (*SyGI*) and *Friendly Boy* (*FrBy*), which are closely linked and located in the sex-determining region (SDR) of the Y chromosome (Akagi et al., 2018, 2019; Varkonyi-Gasic et al., 2021). Conversely, the conservation of *SyGI* and *FrBy* among the genus *Actinidia* has demonstrated that an initial SDR was developed before species divergence, agreeing with the observations on floral morphology across species (Akagi et al., 2023; Yue et al., 2024).

Except for the floral morphology, kiwifruit also exhibit sexual dimorphism in a variety of floral characteristics, such as flower number and flowering time (Cheng et al., 2006; Ferguson, 1991; Testolin, 1991), suggesting a long evolutionary history of antagonistic selection predating species differentiation. Naturally, these SA polymorphisms would be maintained and can be examined in the extant kiwifruit genetic resources. Furthermore, the consistent and conserved patterns of floral dimorphism could indicate that SA selection may have a significant effect on sexual fitness and evolution of reproductive organs in the universal ancestor of kiwifruit. It is well-documented that transposon bursts make great contributions to the rapid expansion of SDR on the Y chromosome during kiwifruit evolution (Akagi et al., 2023; Yue et al., 2024). However, details about the occurrence and influence of SA selection in kiwifruit SDR are still limited.

Pan-genomics is a newly emerging and highly effective tool for assessing the genetic diversity within and/or between populations. Through phylogenetic genome comparison, it enables the detection of genomic sequences and protein-coding genes not present in a single genome. Recently, the first graph-based pan-genome of kiwifruit has been constructed to reveal structural variations mediating fruit de-greening in *Actinidia chinensis*, which could also extend our exploration and characterization of intraspecific genomic diversity in the future (Wang et al., 2024). Meanwhile, an increasing number of published genomes from the genus *Actinidia* offer new opportunities to fully capture interspecific genetic diversity across kiwifruit species by using comparative pan-genome analysis (Han et al., 2023; Liu et al., 2024; Wang et al., 2023; Yao et al., 2022; Yu et al., 2023).

In this study, by collecting 10 high-quality chromosome-scale genome assemblies of 6 kiwifruit genotypes from *A. chinensis* and *Actinidia eriantha*, we constructed a gene-based pan-genome and disclosed millions of gene presence/absence variations (PAVs) and gene copy-number variations (CNVs) that are hard to detect when analyzing single reference genomes (Yue et al., 2023). Benefiting from the inclusion of male genomes, our gene-based pan-genome, when combined with a custom SynPanScan pipeline, allows for in-depth comparative analysis of gene PAVs and CNVs potentially related to SA selection between sexes in kiwifruit. Leveraging this integrated pipeline, we achieved the successful identification of the *Y-linked FT* (*YFT*) gene, which is unique to males and belongs to the *FLOWERING LOCUS T* (*FT*) gene family (Akagi et al., 2018). Phylogenetic analysis provided evidence for robust orthologous relationships of *YFT* across different species and lineage-specific expansion of *FT* after the recent whole-genome duplication (WGD) event in the founding ancestor. The expression pattern of *YFT* in both floral buds and leaves of the male kiwifruit, as supported by transcriptomic analysis, is consistent with its conserved putative role in flowering regulation. Moreover, ectopic expression of *A. eriantha YFT* (*AerYFT*) resulted in considerably earlier flowering in Arabidopsis, which could be indicative of SA selection on flowering time in the process of kiwifruit evolution. The source code, web server, and technical documentation of SynPanScan are publicly available at https://synpanscan.atcgn.com/.

RESULTS

Phenotypic observation of kiwifruit flowering time

To validate the observed differentiation of kiwifruit flowering time between sexes, we have maintained long-term phenological records of flowering dates for over 280 adult vines with a female-to-male sex ratio of 1.04:1 in an intraspecific hybrid population of *A. eriantha* during the flowering season in 2024. The flowering time for each vine was recorded as the date on which the first fully open flower was observed. On May 9, we observed multiple opening flowers on six individual male vines (Figure 1a). In contrast, our observation revealed a 1-day delay in female flower opening, with the first fully open flower appearing on May 10 (Figure 1b). Notably, at the 10-day observation point, all female vines had completed flowering and entered the senescence phase, whereas one male vine still retained open flowers.

Globally, the flowering phenology of our hybrid population, in both males and females, is well approximated by a normal distribution (Figure 1c). Through further comparison, the mean flowering time of male vines (3.67 days after May 9) is significantly earlier than that of female vines (4.82 days after May 9) with Student's *t*-test (*P*-value < 0.001), confirming our observation of sexual dimorphism in flowering time (Figure 1d). Meanwhile, male vines have a relatively longer flowering period than female vines (11 versus 9 days). In addition, the standard deviation of females (1.69) in flowering time is smaller than that of males (1.90), reflecting that the female population has a more synchronized flowering period (Figure 1c). Therefore, these data provide evidence for the outcomes of

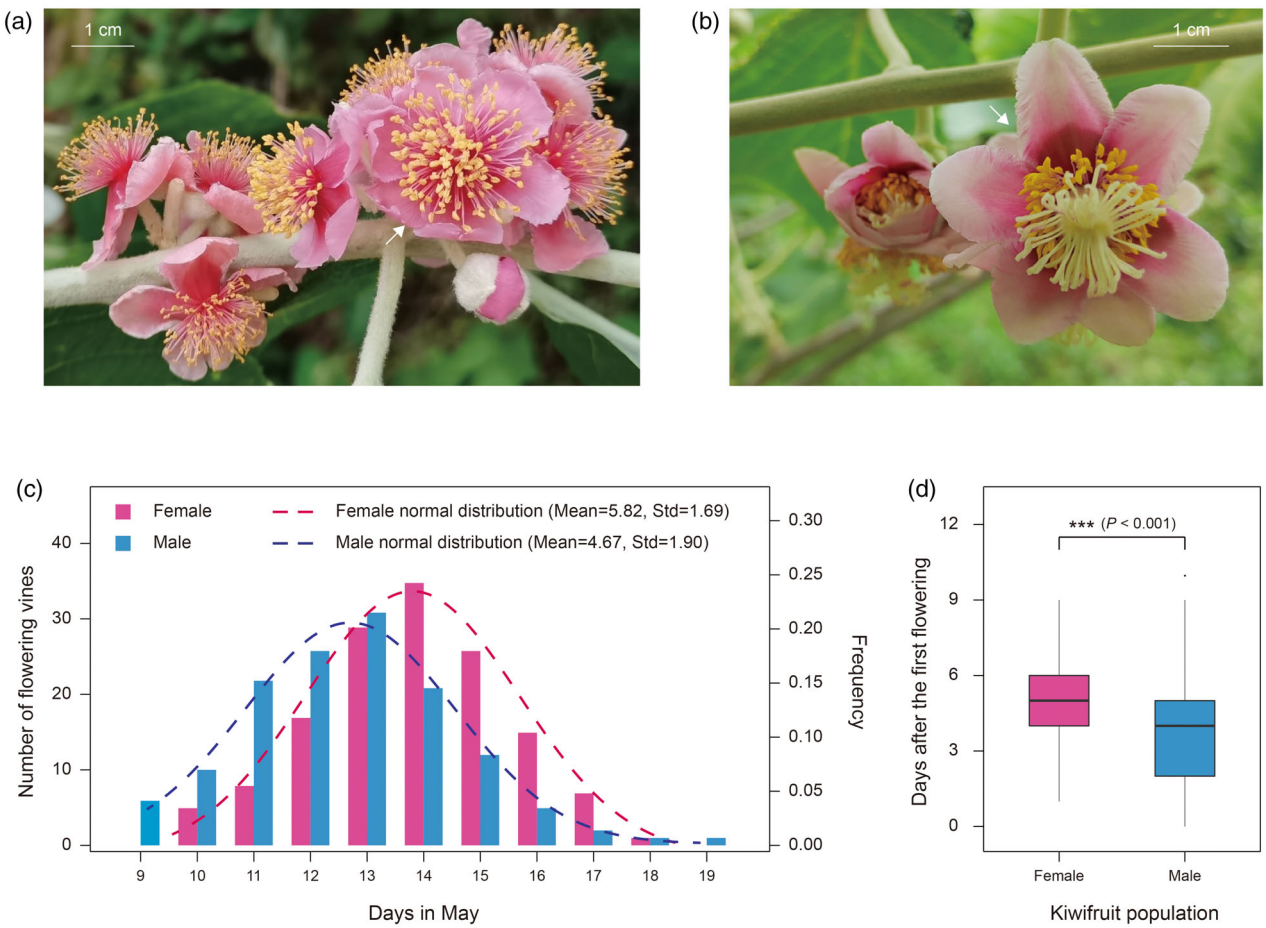

Figure 1. Phenotypic observation of flowering time in males and females of adult kiwifruit vines.
(a) Male floral morphology. Arrow marks a fully open flower.
(b) Female floral morphology. Arrow marks a fully open flower.
(c) Statistics of flowering time for a total of 143 female and 137 male vines in our hybrid population. Their respective normal distribution is used to estimate the mean and the standard deviation.
(d) The boxplots showing the number of days after the first flowering for all the male and female vines, respectively. Statistical significance was determined by Student's *t*-test (***P*-value < 0.001). Sample sizes: female vines, *n* = 143; male vines, *n* = 137.

evolutionary mechanisms that underpin sexual adaptation in kiwifruit.

Gene-based pan-genome construction of the genus *Actinidia*

To identify genetic determinants underlying the observed flowering time dimorphism, we first conducted a comprehensive pan-genome analysis of the genus *Actinidia*, which enables simultaneous discovery of both novel non-reference loci and functionally constrained genes across species. By clustering 457 899 predicted genes from the 10 genome assemblies of *A. chinensis* and *A. eriantha* (Table S1), we constructed a protein-coding gene-based super pan-genome for kiwifruit, which resulted in a total of 52 774 non-redundant pan-gene orthogroups comprising 42 370 gene clusters and 10 404 unassigned genes (Table S2). Based on the distribution of these pan-gene orthogroups in all assemblies, 19 230 (36.4%) orthogroups were categorized as core pan-genes (genes present in all 10 assemblies) and 33 544 (63.6%) orthogroups were categorized as dispensable pan-genes (genes absent in at least one assembly) (Figure 2a). These dispensable pan-genes were further divided into 3967 (7.5%) softcore (genes in those orthogroups present in more than 80% assemblies), 129 (0.2%) cloud (genes in those orthogroups with two or more members of a given gene cluster present in only one assembly), 10 404 (19.7%) unassigned (genes in those orthogroups with a sole member present in only one assembly) and 19 044 (36.1%) shell (genes in the rest orthogroups) orthogroups according to their presence in each assembly (Figure 2a,b). On average, each individual kiwifruit genome assembly consisted of 69.2, 10.4, 18.1, 0.1, and 2.3% genes from the core, softcore, shell, cloud, and unassigned orthogroups in our constructed gene-based pan-genome (Figure 2c; Table S3). The results of simulating pan-gene size indicated that when the number of assemblies exceeds eight, the number of both total pan-gene orthogroups and core pan-gene orthogroups approaches stability, suggesting that the constructed pan-genome has reached saturation (Figure 2d). Specifically, an average of just three new pan-gene orthogroups were obtained when adding the 10 assembly (Table S4), further indicating the representation of the six kiwifruit cultivars or lines selected in our study.

In comparison, the sequence lengths and expression levels of core pan-gene orthogroups were significantly greater than those of dispensable pan-gene orthogroups (Figure 2e,f; Table S5), which suggested that the core pan-genes may play more general roles in the developmental process of kiwifruit. Conversely, the non-synonymous/synonymous substitution ratio (K_a/K_s) of core pan-gene orthogroups was smaller than that of dispensable pan-gene orthogroups, indicating that the core pan-genes are subject to strong selective pressure and the dispensable pan-genes have undergone less stringent purifying selection (Figure 2g; Table S6). Furthermore, functional enrichment analysis based on gene ontology (GO) annotation also indicated that core pan-genes were enriched for several essential biological processes and molecular functions such as positive regulation of transcription, DNA-templated (GO:0045893, *P*-value < 0.001), transcription regulatory region sequence-specific DNA binding (GO:0000976, *P*-value < 0.001), protein binding (GO:0005515, *P*-value < 0.001), and transcription coactivator activity (GO:0003713, *P*-value < 0.01) (Table S7), while dispensable pan-genes were significantly involved in primary and secondary metabolism activities including carbohydrate metabolic process (GO:0005975, *P*-value < 0.001), gluconeogenesis (GO:0006094, *P*-value < 0.001), serine family amino acid metabolic process (GO:0009069, *P*-value < 0.001), and sucrose metabolic process (GO:0005985, *P*-value < 0.001) (Table S8). Together, all these findings strongly demonstrated that core pan-genes are comparatively conserved among the genus *Actinidia*, whereas dispensable pan-genes exhibit higher genetic variations and faster evolutionary rates to acquire new functions for the adaptation of different kiwifruit species to diverse environmental conditions or selection pressures.

Comparative pan-genome analysis of male and female kiwifruit

With a pan-genome developed, we then conducted comparative analyses to link genetic variations, such as PAVs and CNVs, to specific phenotypic differences, thereby identifying a core set of features common across all predefined subgroups. The male–female pan-genome serves as a powerful framework to directly investigate inter-sex genomic variations and ultimately infer candidate loci that have been shaped by sexual antagonistic selection over kiwifruit evolutionary history. Furthermore, syntelog is devoted to describing the type of homology where genes involved are derived from the same ancestral source (Wu et al., 2023). Therefore, the integration of synteny-based anchoring and pan-genomic clustering can help trace lineage-specific adaptive evolution at both large scales and high details. For this purpose, we have developed a custom pipeline, Synteny-based Pan-genomic Scan (SynPanScan), to specifically screen syntenic genes through the comparative analysis of our constructed gene-based pan-genome (see Experimental Procedures).

Using the SynPanScan pipeline, we identified 657 syntenic gene sets exhibiting sex-differentiated PAVs and CNVs from a total of 595 pan-gene orthogroups, representing the deeply conserved ancestral characters shared by all the extant kiwifruit species (Table S9). Among them, 240 gene sets were always present in males but entirely absent in females (hereafter called male-specific category and abbreviated MS) and 88 gene sets that were only present

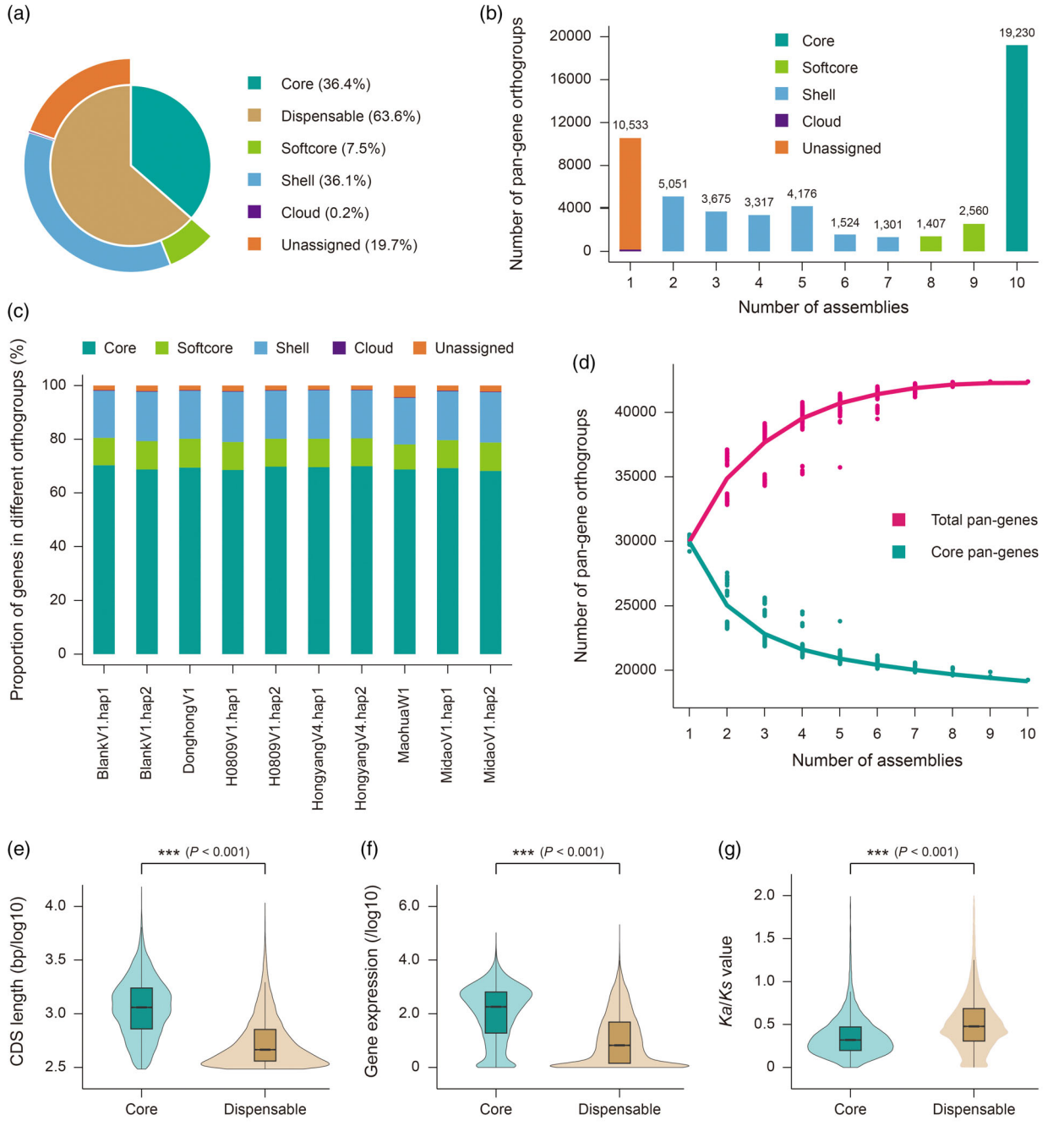

Figure 2. Characterization of the constructed kiwifruit gene-based pan-genome.
(a) Proportion of core, softcore, shell, cloud, and unassigned pan-gene orthogroups in the pan-genome.
(b) Number of pan-gene orthogroups distributed among the 10 genome assemblies.
(c) Composition of core, softcore, shell, cloud, and unassigned pan-gene orthogroups in each genome assembly.
(d) Statistics of the total and core pan-gene orthogroups along with an increasing number of the genome assemblies.
(e) Violin plots showing the difference of CDS length between the core and dispensable pan-gene orthogroups.
(f) Violin plots showing the difference of gene expression between the core and dispensable pan-gene orthogroups.
(g) Violin plots showing the difference of *Ka*/*Ks* values between the core and dispensable pan-gene orthogroups. Statistical significance was determined by Student's *t*-test (***P-value < 0.001). Sample sizes: core pan-genes, n = 19 229; dispensable pan-genes, n = 23 142.

in the four female genomes (hereafter called female-specific category and abbreviated FS). For distinction, the rest of 17 and 312 gene sets were respectively defined as male-biased (hereafter abbreviated MB) and female-biased (hereafter abbreviated FB) categories in the pan-genome under a statistically significant threshold (P-value < 0.05). It

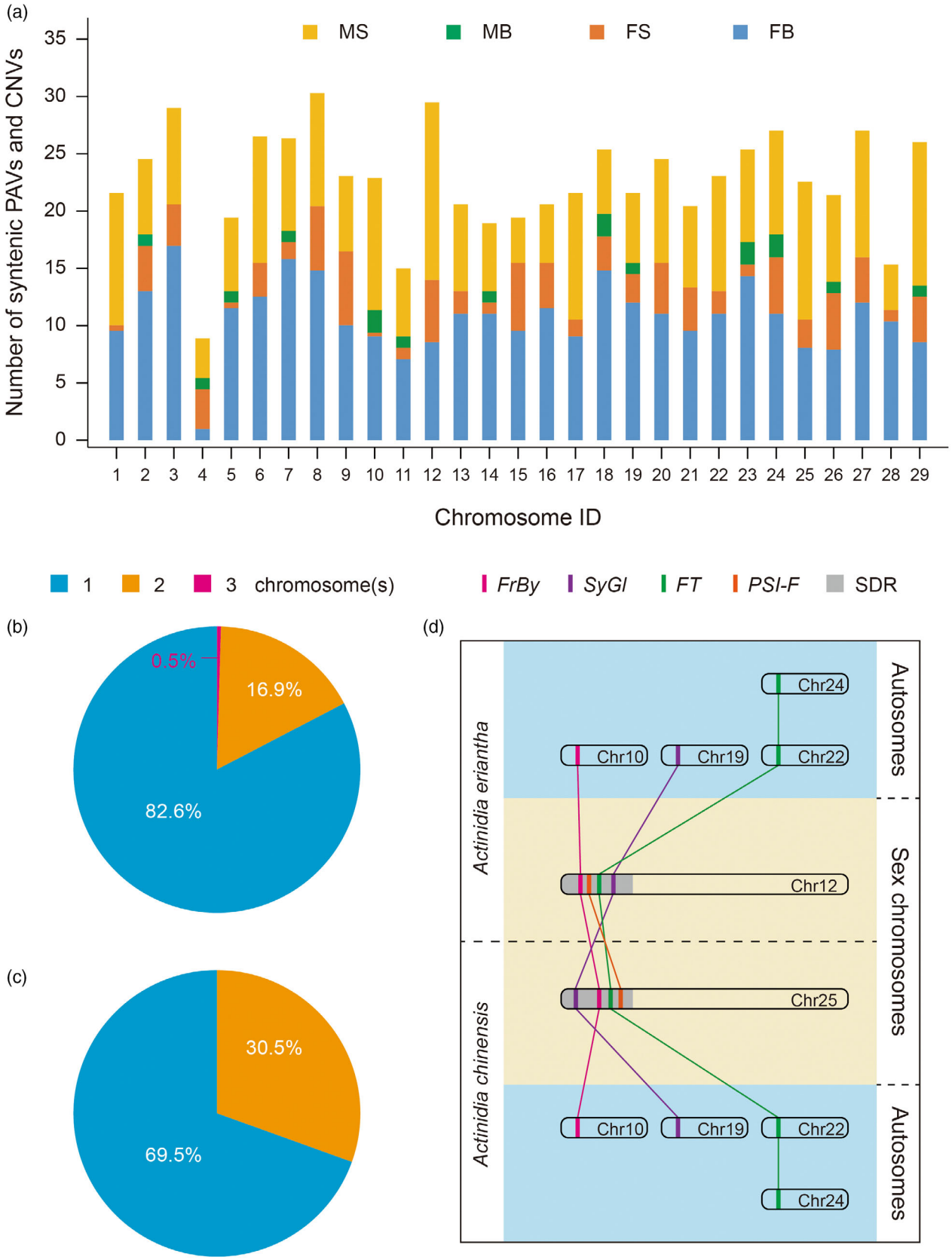

Figure 3. Identification and characterization of annotated genes from syntenic gene sets exhibiting sex-differentiated occurrence in the kiwifruit pan-genome.
(a) Chromosomal distribution of the identified gene sets in the male-specific (MS), male-biased (MB), female-specific (FS), and female-biased (FB) categories.
(b) Composition of all the gene sets based on the number of chromosomes where individual genes are located.
(c) Composition of those gene sets related to sex chromosomes based on the number of chromosomes where individual genes are located.
(d) Schematic diagram showing the syntelogous genes between two sex chromosomes of *Actinidia chinensis* (Chr25) and *Actinidia eriantha* (Chr12). The orthogroups of *FrBy*, *SyGI*, and *FT* are identified as core pan-genes, and *PSI-F* is a PAV gene belonging to the shell pan-gene orthogroups. Their homologous members located on autosomes are also presented.

is observed that males and females exhibit distinct preferences for genetic variations, whereas males tend to carry unique evolutionary signatures and females show relevant population biases.

Notably, the number of syntenic gene sets on each chromosome was analyzed, revealing distinct chromosomal distribution patterns among the four categories of inter-sexual PAVs and CNVs (Figure 3a). As expected, the MS category appeared to be preferentially distributed on chromosomes 12 and 25, which are the sex chromosomes of *A. eriantha* and *A. chinensis*, respectively. In contrast, the genomic location of the FB category showed a possible link with the chromosome length, where the highest number of gene sets was found on chromosomes 3 and 7 ($r = 0.62$, P-value <0.001) (Table S10). Additionally, the comparison of genomic location for individual genes indicated that the majority of sex-differentiated gene sets are located on the same chromosomes among different genome assemblies, accounting for 82.6% (543 in 657) (Figure 3b). The rest are dispersed on multiple chromosomes, consisting of 16.9% (111 in 657) and 0.5% (3 in 657) on two and three chromosomes, respectively (Figure 3b).

Furthermore, we focused on those genes located on the sex chromosomes (Chr12 in *A. eriantha* and Chr25 in *A. chinensis*) and found a total of 59 syntenic gene sets (Table S9). Among these, 41 syntenic gene sets were formed by genes from the same chromosomes, accounting for 69.5% (Figure 3c), which was slightly below the global averaged value of 82.6%. On the contrary, 18 gene sets (~30.5%) were composed of syntelogous genes from two different chromosomes (Figure 3c), indicating a higher frequency of inter-chromosomal translocations between sex chromosomes and/or ordinary autosomes in kiwifruit. It is of interest that in the MS category, there were four pairs of syntelogous genes presented between the two sex chromosomes of *A. chinensis* and *A. eriantha* (Figure 3d). Comparative genome annotation showed that these syntelogous genes were all unique to males and located within the SDRs of Y chromosomes. Among them, two gene pairs are *SyGI* and *FrBy*, which are well-characterized sex-determining genes, and the other two pairs are predicted to be genes encoding FT and photosystem I reaction center subunit III (PSI-F) (Table S5). On the basis of our constructed pan-genome, the orthogroups of *FrBy*, *SyGI* and *FT* are identified as core pan-genes, whereas PSI-F, belonging to the shell pan-gene orthogroups, is a PAV gene that exists only in the males of kiwifruit. Together, the successful identification of these established regulators demonstrates the high accuracy and integrity of our SynPanScan pipeline.

Genetic diversity assessment of the kiwifruit *FT* gene family

Based on genome annotation, the *FT* gene family of kiwifruit comprises four members in males and three in females, which are divided into two pan-gene orthogroups in our constructed pan-genome. One is designated as OG002159, which includes *YFT*, *FT1*, and *FT2*; the other is OG021078, which comprises the *FT-like* genes only. As mentioned above, the syntenic gene set of *YFT* involved in the MS category is part of its cognate pan-gene orthogroup, showing evidence of lineage-specific paralog retention following WGD in both *A. chinensis* and *A. eriantha*. Phylogenetic analysis further confirmed that the two *YFT* genes in the MS category are orthologous (Figure 4a), suggesting they are derived from a single ancestral gene in the evolutionary process. Meanwhile, all those genes from autosomes (Chr22 and Chr24) could be classified into three distinct subfamilies, which are respectively homologous to *FT1*, *FT2*, and *FT-like* as previously characterized (Voogd et al., 2017). This mode of separation indicated that *FT1*, *FT2*, and *FT-like* were also formed in the kiwifruit ancestor and then inherited by vertical transmission during the process of speciation.

To explore the evolutionary history of the *FT* gene family, we calculated the values of sequence similarity, synonymous substitution (*Ks*) and non-synonymous substitution (*Ka*) between or within the subfamilies of *YFT*, *FT1* and *FT2* in all genomes of *A. chinensis* and *A. eriantha* (Table S11). Accordingly, each of the three subfamilies has an extremely high sequence similarity, showing unusual evolutionary conservation among different kiwifruit species (Figure 4b). In comparison, *YFT* has a higher sequence similarity with *FT2* than with *FT1*, suggesting that it may be a direct duplication of *FT2* (Figure 4b). The *Ks* value between *YFT* and *FT2* ($Ks = 0.060$) indicated that their duplication occurred after the recent WGD event (α) but before different kiwifruit species divergence (Figure 4c,e). Meanwhile, the *Ks* value between *FT1* and *FT2* ($Ks = 0.198$) indicated that this lineage-specific gene duplication occurred before the recent WGD event (α) but after the ancient WDG event (β) in kiwifruit ancestor (Figure 4c,e). Additionally, the *Ka*/*Ks* values of *YFT*, *FT1*, and *FT2* were all smaller than one, demonstrating that they have been

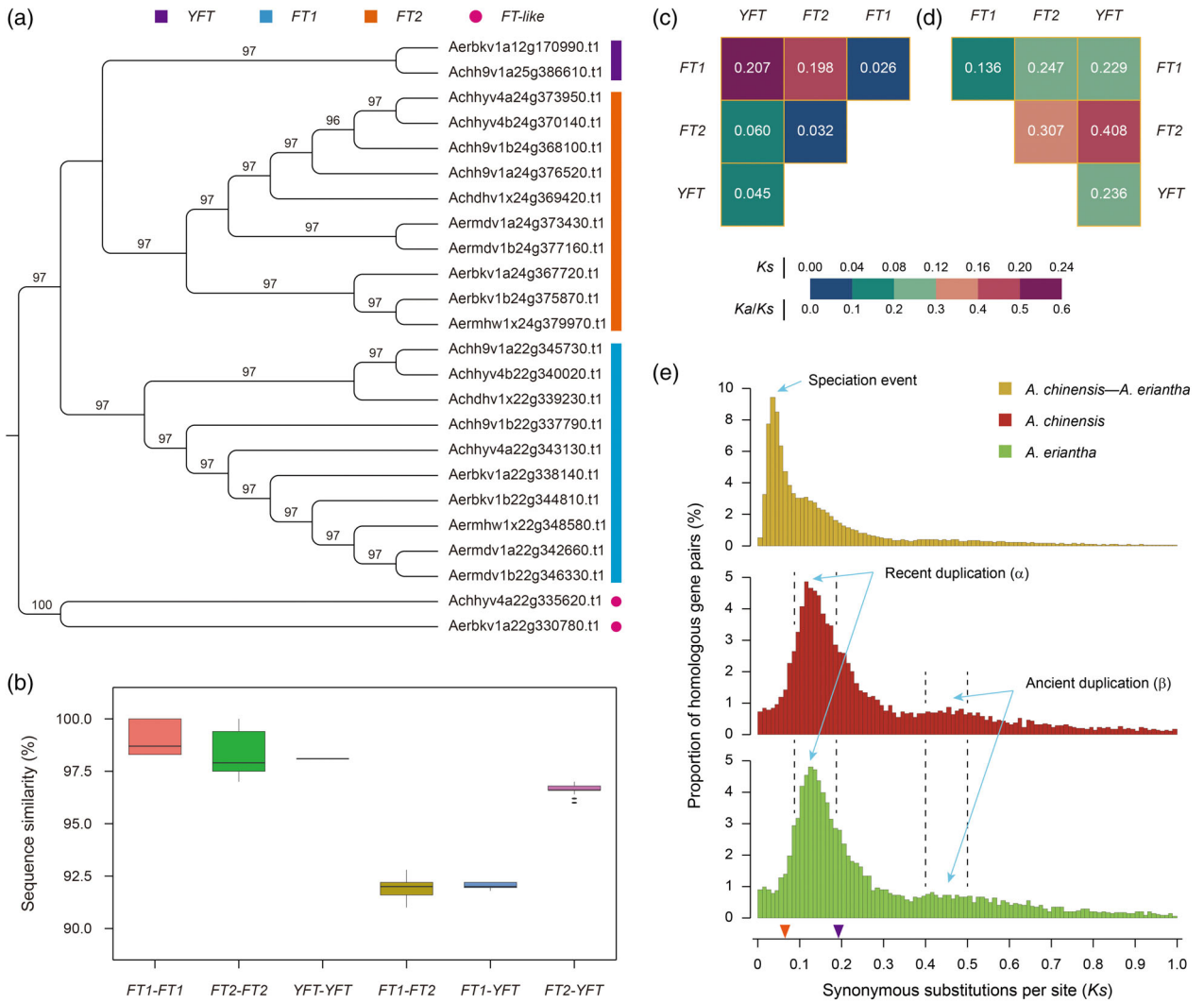

Figure 4. Genetic diversity and evolution of the kiwifruit *FT* gene family.
(a) Phylogenetic tree of the *FT* gene family consists of *YFT*, *FT1*, *FT2*, and *FT-like*. The *FT-like* genes of BlankV1.hap1 and HongyangV4.hap1 are used as an outgroup. The chromosomal locations of *AerYFT* and *AchYFT* are different due to the turnover of sex chromosomes between species.
(b) The average values of sequence similarity between or among each *FT* subfamily.
(c) The average values of *Ks* between or among each *FT* subfamily.
(d) The average values of *Ka*/*Ks* between or among each *FT* subfamily.
(e) The two whole-genome duplication events detected in *Actinidia chinensis* and *Actinidia eriantha* as well as the speciation event of *A. chinensis* and *A. eriantha*. Arrows on the *x*-axis indicate the *Ks* values for the *YFT* versus *FT2* pair (Orange arrow, *Ks* = 0.060) and the *FT1* versus *FT2* pair (Purple arrow, *Ks* = 0.198), respectively.

under strong purifying selection (Figure 4d). Interestingly, *FT1* has the lowest *Ka*/*Ks* value, while *FT2* has the highest among the three subfamilies. This probably suggested that *FT1* is functionally more conserved with a stronger purifying selection than *FT2* in kiwifruit.

Functional characterization of *YFT* in accelerating flowering

As protein function is closely associated with protein sequence, we performed multiple alignments of full-length coding sequences for the whole *FT* gene family. The results reflected a high amino acid sequence similarity ranging from 88.5 to 100% among all the identified FT1, FT2, and YFT proteins (Table S11). Like FT1 and FT2, YFT also has the conserved PEBP domains (DPDxP and GxHR) and key amino acid residues (Y84 and Q139), which are essential for FT's biological function (Figure 5a). Meanwhile, YFT possesses a conserved 14-residue external loop (LGRQTVYxPxWRQN) in segment A, a signature motif shared among flowering-inducer FT proteins, supporting its role as a floral activator. Furthermore, the LYN motif, which ensures the requirement of

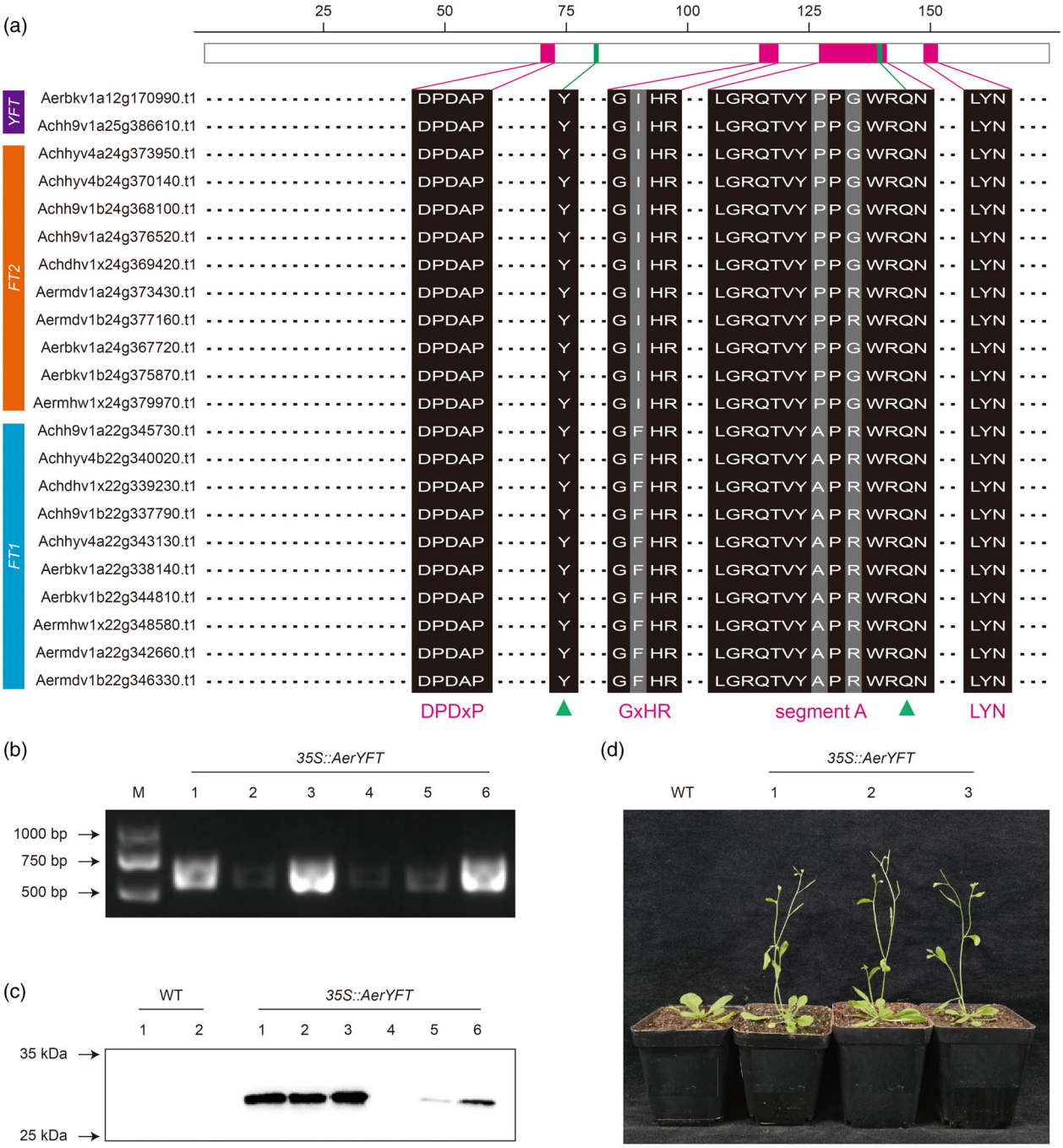

Figure 5. Functional conservation of *YFT* in accelerating flowering.
(a) Amino acid sequence alignments of *YFT*, *FT1*, and *FT2*. Only the positions and domains critical for protein function are partially displayed. Conserved sites are indicated in black (the best alignment) or gray (the next best alignment).
(b) Each transgenic line with *AerYFT* is individually tested by PCR assay.
(c) The ectopic expression of AerYFT protein in each T1 transgenic line is confirmed by Western immunoblotting.
(d) Earlier flowering was observed in transgenic *35S::AerYFT* lines compared with wild-type controls. Shown are representative phenotypes of wild-type (left) and transgenic (right) Arabidopsis plants photographed at 23 days after sowing.

full functionality of the external loop, is also found in YFT, suggesting a conserved activation mechanism (Figure 5a).

To assess whether *YFT* could alter the flowering time, we have explored the effects of ectopically expressed *A. eriantha YFT* (*AerYFT*) in transgenic Arabidopsis plants.

The coding sequence of *AerYFT* driven by the CaMV *35S* promoter (*35S::AerYFT*) was introduced into wild-type Col-0 and its presence was checked by PCR amplification for a couple of independent lines (Figure 5b). The ectopic expression of AerYFT protein in each T1 transgenic line was confirmed by Western immunoblotting with a monoclonal HA antibody (Figure 5c). The first three lines showing high expression of AerYFT protein were monitored for flowering time.

As expected, we could clearly observe the accelerated flowering in all T2 transgenic Arabidopsis plants. The flowering time of transgenic lines was recorded at 23 days, on average, which was significantly shorter than the 30 days determined for wild-type lines through continuous observation of their entire growth cycle (Figure 5d). Together, these results demonstrate that the constitutive expression of *AerYFT* promotes early flowering in Arabidopsis, confirming that AerYFT acts as a functionally conserved floral activator, similar to the previously characterized kiwifruit FT proteins, FT1 and FT2. Furthermore, the endogenous role of *YFT* is supported by its high expression levels in both floral buds and leaves of male kiwifruit during the flowering period (Figure S1). This expression pattern is characteristic of a canonical florigen gene involved in flowering regulation.

DISCUSSION

Plants have built-in mechanisms to precisely control the flowering time by integrating developmental and environmental cues (Yang et al., 2018). The *FT* gene family is well known as a master flowering regulator and has emerged with the evolution of flowering plants (Wickland & Hanzawa, 2015; Yu et al., 2025). Among angiosperms, *FT* homologs exhibit a universally conserved function of promoting the transition to reproductive development and flowering. However, identification of multiple *FT* paralogs in a number of annual and perennial species has suggested their functional diversification in plant growth and development (Blackman et al., 2010; Jiang et al., 2022; Navarro et al., 2011; Zheng et al., 2023). In kiwifruit, a total of three *FT* genes were previously identified, which are able to promote flowering when ectopically expressed in Arabidopsis and kiwifruit (Moss et al., 2018; Varkonyi-Gasic et al., 2013; Voogd et al., 2017). Among them, *FT1* and *FT2* showed a much higher degree of sequence similarity than *FT-like*, which can also be seen in our gene-based pan-genome: *FT1* and *FT2* were clustered into the same orthogroup, whereas *FT-like* represented a separate orthogroup due to the relatively lower sequence identity (Table S11). These results demonstrate that the construction of super pan-genome is a powerful approach for resolving broad-scale genetic diversity in more detail than a single reference genome. Through comparative analysis, we have identified a male-specific, SDR-located *YFT* gene, which is clustered with *FT1* and *FT2* in the same orthogroup, as a key factor underlying the earlier flowering phenotype in male kiwifruit plants.

It is well known that WGD is the major driving force for gene family expansion in both plants and animals. Our analyses demonstrate that the expansion of the *FT* gene family was entirely attributed to three successive WGD events, including one ancient hexaploidization event (γ) and two recent diploidization events (α and β) (Huang et al., 2013). Phylogenetically, the duplication of *FT1* and *FT-like* most likely occurred following the γ event shared by core eudicots, which could also be consolidated in grape (Jaillon et al., 2007), sunflower (Mota et al., 2016), lettuce (Reyes-Chin-Wo et al., 2017), and Asteraceae (Kong et al., 2023). Furthermore, kiwifruit has undergone two additional independent WGD events after the divergence from plant lineages that include sequenced genomes such as tomato and potato (Huang et al., 2013). These duplications could give rise to the neofunctionalization of genes responsible for key kiwifruit traits. Here, we present evidence that *FT2* and *YFT* were derived from the recent β and the most recent α events, respectively. After duplication, *FT-like* may well maintain the ancestral flowering control function due to its highly conserved sequence among the genus *Actinidia*. On the other hand, *FT1* was free to accumulate genetic variations toward a potentially new function, which has also become the starting point for gene sequence evolution of *FT2* and *YFT*. Although the molecular functions of *FT1*, *FT2*, and *YFT* were nearly identical, their biological roles were divergent by acquiring different patterns of gene expression and/or hemizygous variations in kiwifruit (Akagi et al., 2018; Voogd et al., 2017; Yue et al., 2024). Taken together, we propose a working hypothesis that the basic flowering framework for *Actinidia* is primarily established by *FT1* and *FT2*, while the flowering time differential between males and females is fine-tuned by *YFT*.

The development of unisexual floral organs is almost synchronous, but still shows a slight difference in flowering time between males and females. In theory, the occurrence and maintenance of sexual dimorphism are generally subjected to SA selection and genetically controlled by SA genes during evolution (Kaufmann et al., 2023). Here, we have focused on *YFT* and its potential role in mediating sexual dimorphism of flowering time in kiwifruit. Notably, *YFT* clustered together with *FT1* and *FT2* to form a closely linked clade, suggesting their conserved functions on the molecular control of kiwifruit floral induction. Moreover, *YFT* isolated from *A. eriantha* was ectopically expressed in Arabidopsis and induced early flowering, consistent with prior studies across diverse plant species (Abdulla et al., 2024; Song et al., 2019; Sun et al., 2017; Wan et al., 2024). These data are consistent with the functionality of *YFT* in the control of flowering

time. Specifically, the male-specific presence and development-specific expression of *YFT* could lead to a sex-dependent biological role in kiwifruit, with males exhibiting an extended flowering period compared with females (Figure 1). Therefore, it is possible that *YFT* contributes to the observed sexual dimorphism in flowering time within the genus *Actinidia*.

The difference of male–female synchrony occurring in nature could be of great significance, for it has been proposed that an extended flowering window can enhance male reproductive success by increasing pollen output and dispersal opportunity. Another reproductive strategy to enhance pollen export efficiency is the increase of flower number per male vine, which is attributed to the pleiotropic effects of *SyGI* in kiwifruit (Akagi et al., 2023). Unlike *SyGI*, a primary sex-determining gene suppressing gynoecium development, *YFT* may be specifically involved in the regulation of male flowering time. This distinction highlights the presence of dedicated SA genes within the SDR, providing important new evidence that expands upon published findings (Akagi et al., 2023). Perhaps, *SyGI* and *YFT* have achieved spatiotemporal coordination to optimize male reproductive fitness: *SyGI* determines flower number in the spatial term, while *YFT* controls flowering time in the temporal term.

Furthermore, early flowering confers male fitness advantages through competitive precedence in pollination according to Bateman's principle (Brown et al., 2009). Although male pollen contributes nothing to female fitness, it has to compete with each other for fertilization opportunities, especially if hermaphrodite pollen is available (Spencer & Rieseberg, 1995; Wang et al., 2021). From the perspective of females, early male flowering can ensure continuous pollen availability. Even with some pollen loss, the mechanism achieves markedly higher fertilization efficiency for the much more precious female ovules. Consequently, the different reproductive requirements of males and females provide an explanation for why female individuals do not need *YFT* to flower earlier but evolve this kind of sexually dimorphic trait in the ancestral evolutionary process of kiwifruit. On the other hand, flowering time between males and females cannot differ too much to avoid unsuccessful mating (Janzen, 1977). Thus, the slightly asynchronous flower development in kiwifruit should be a balancing act that has been carefully shaped through the adaptive evolution of increased both male and female fitness.

It is worth noting that the rise of sexual dimorphism and SA selection coincides with the evolution of sex chromosomes. In kiwifruit, sex chromosomes are determined by the SDR that carries two sex-determining genes, *SyGI* and *FrBy* (Akagi et al., 2018, 2019). Our analyses show that the duplication time of *YFT* was almost the same as *SyGI* and *FrBy*, suggesting the antagonistic selection on flowering time has been completed soon after the formation of the initial SDR in kiwifruit ancestor. Remarkably, *YFT* embedded into the SDR of the Y chromosome can be beneficial to its spread and fixation in natural populations. Beyond this, our comparative pan-genome analysis revealed a high frequency of inter-chromosomal translocations involving the sex chromosomes, consistent with models positing that recombination suppression creates a permissive environment for structural variation accumulation. Moreover, we also identified multiple candidate SA genes on autosomes, indicating their potential contributions to sexually dimorphic traits beyond the sex chromosomes. One explanation for this finding is that there is likely to be a coordinated set of interactions between the autosomal genes and SDR-encoding genes (Kaufmann et al., 2021; Zheng & Xia, 2022). But in the long-run evolution, autosomal genes under SA selection would facilitate the linkage to the existing sex-determining genes or the development of novel sex-determining genes, thus leading to the expansion of SDRs or the turnover of sex chromosomes in kiwifruit.

Nevertheless, we cannot empirically reconstruct the ancestral genetic architecture of sexual dimorphism, as sex chromosomes evolved rapidly following kiwifruit species divergence. Alternatively, we make an exploratory attempt by utilizing the advantage of synteny-based super pan-genome in evolutionary studies. At the genus level, comparative analyses of gene PAVs and CNVs could identify sex-specific and sex-biased syntenic gene sets shared by the extant kiwifruit species, representing the ancestral characters responsible for sexual dimorphism that have undergone positive selection during evolution. Our attempts demonstrate that synteny-based anchoring and pan-genomic clustering could complement each other due to their respective advantages, providing a robust approach for tracing inter-group divergence. The SynPanScan pipeline is capable of analyzing both sexual dimorphism and any other significantly divergent traits across species. As an increasing number of genomes and pan-genomes are released, SynPanScan can represent a significant advance over previous works that rely on massive resequencing of population samples through in-depth mining of publicly available data (Delph et al., 2022; Svensson et al., 2018). Furthermore, to enhance user accessibility, we have developed both a standalone local application and a web service for SynPanScan.

CONCLUSION

This study deciphers the genetic architecture of plant sexual dimorphism by using synteny-based comparative super pan-genome analysis. Within the *FT* gene family, we have identified *YFT* as a key regulator of both sexual dimorphism and SA selection in flowering time during kiwifruit evolution. The location of *YFT* in the SDR not only

facilitates its spread in natural populations but also promotes the expansion of SDR on the Y chromosome. Moreover, our findings also cast new light on the mystery of why sex chromosome turnover frequently occurs in kiwifruit.

EXPERIMENTAL PROCEDURES

Plant materials and growth conditions

For gene clone of the *YFT* sequence, fresh young healthy leaves were collected from a male cultivar, *A. eriantha* 'Blank'. For phenotypic observation of the flowering time, an intraspecific hybrid population of *A. eriantha* over 4-year periods was constructed and assessed. All kiwifruit vines were grown in the orchard under natural conditions and standard practice. On the other hand, the ecotype Columbia-0 (Col-0) of *Arabidopsis thaliana* (Arabidopsis) was used as wild-type plants in our transgenic study. Arabidopsis plants were grown in a chamber at 23°C under long-day condition (16-h light/8-h dark cycles) with 40–60% humidity.

Monitoring of flowering phenology

Flowering phenology was monitored and recorded for each individual vine throughout the entire flowering season. To ensure that transient flowering events were accurately captured and not overlooked, observations were conducted daily. On each day of assessment, monitoring was performed during a fixed time window (between 9:00 and 11:00) to standardize observations and coincide with the peak floral activity. This daily, timed protocol allowed for the reliable documentation of key flowering statistics, including the date of first bloom, full bloom, and the end of bloom for every vine in the population.

Construction of gene-based pan-genome

To construct the gene-based pan-genome, we used OrthoFinder (Emms & Kelly, 2019) to cluster the protein-coding genes from *A. chinensis* 'Donghong' (DonghongV1) (Han et al., 2023), *A. chinensis* 'H0809' (H0809V1) (Yue et al., 2024), *A. chinensis* 'Hongyang' (HongyangV4) (Yue et al., 2023), *A. eriantha* 'Blank' (BlankV1) (Yue et al., 2024), *A. eriantha* wild material (MaohuaW1) (Yao et al., 2022), and *A. eriantha* 'Midao' (MidaoV1) (Wang et al., 2023). All the data were downloaded from the KPGD database (Li et al., 2025). Among them, H0809V1 and BlankV1 were sequenced from the male kiwifruit plants. Gene families shared by all the 10 assemblies are defined as the core pan-gene orthogroups, whereas the ones that are missing in one or more assemblies are considered to be the dispensable pan-gene orthogroups. The dispensable pan-gene orthogroups are further categorized into the softcore (genes in those orthogroups present in more than 80% assemblies), cloud (genes in those orthogroups with two or more members of a given gene family present in only one assembly), unassigned (genes in those orthogroups with a sole member present in only one assembly), and shell (genes in the rest orthogroups) orthogroups. To estimate the sizes of pan-genome and core-genome, the expected dataset was generated by 1000 simulations for every number from 1 to 10.

Development of the SynPanScan pipeline

The SynPanScan pipeline consists of the following five steps (Figure S2A): (1) extraction of the longest protein isoforms from each genome assembly; (2) construction of gene-based pan-genome through OrthoFinder (Emms & Kelly, 2019); (3) detection of synteny blocks using MCScanX (Wang et al., 2012); (4) achievement of synteny-based pan-genome by integrating collinear genomic regions from the constructed pan-genome; and (5) identification of significant inter-group variations using the Mann–Whitney *U* test. Collectively, these steps are all implemented in our Perl-based SynPanScan pipeline, which is publicly available at https://synpanscan.atcgn.com/download. For enhanced usability, we have also developed a user-friendly web server, freely accessible at https://synpanscan.atcgn.com/ (Figure S2B). Both the command-line and web-based interfaces require only three input files to execute the analysis (Additional implementation details are documented in the online manual). Once completed, users can efficiently retrieve detailed results using sortable tables and exportable reports (Figure S2C).

Availability and implementation of SynPanScan

SynPanScan is accessible through an intuitive online web server and is also available as a local version for offline, high-performance computing. It was developed in Perl (v5.22.2) with dependencies including BLAST+ (v2.6.0), DIAMOND (v0.9.23), MCScanX (v1.0.0), and OrthoFinder (v2.2.7). The required input files are genome sequences and their corresponding annotations in PEP (protein) and GFF formats. The SynPanScan online web server, local software, detailed tutorials, and usage examples are all accessible at: https://synpanscan.atcgn.com/. Notably, the local version is lightweight and can be run on standard computers without special server requirements.

Analysis of gene synteny

First, the comparisons between genome assemblies were performed by DIAMOND (Buchfink et al., 2021). Then, MCScanX (Wang et al., 2012) was introduced to identify syntenic blocks by using the aligned results of DIAMOND. Any genes within those groups of OrthoFinder and syntenic blocks of MCScanX at the same time were supposed to be syntenic gene sets. Finally, a custom Perl script integrated in the SynPanScan pipeline was used to extract the syntelogous genes.

Construction of phylogenetic tree

All the protein sequences of *FT1*, *FT2* and *YFT* were aligned by the ClustalW tool (version 2.1) (Larkin et al., 2007) and the maximum likelihood phylogenetic tree was constructed by the MEGA tool (version 11) (Tamura et al., 2021) using the neighbor-joining method. The bootstrap process was replicated 1000 times. The protein sequences of *FT-like* from *A. eriantha* 'Blank' (Yue et al., 2024) and *A. chinensis* 'Hongyang' (Yue et al., 2023) were used as an outgroup in our evolutionary tree. Their pairwise sequence alignments were performed by using the EMBOSS Needle program (v6.6.0.0) with parameters (-gapopen 10 -gapextend 0.5) (Madeira et al., 2024).

Calculation of divergence time

The values of *Ks*, *Ka*, and *Ka*/*Ks* for each gene pair were calculated based on the NG (Nei & Gojoberi) method implemented in the PAML program (version 4.9) (Yang, 2007). By using the obtained paralogous gene pairs, we aimed to detect the WGD events according to their *Ks* distribution. The peak *Ks* value was further converted to the divergence time by using the equation $T = Ks/2\lambda$, where λ is the substitution rate of 6.5×10^{-9} mutations per site per year (Yang et al., 2008). The divergence time between *A. chinensis* and *A. eriantha* was calculated by using orthologous gene

pairs between H0809V1.hap1 and BlankV1.hap1 with the same methods.

Comparative transcriptomic analysis

Expression profile analysis of *YFT* was conducted by mapping 20 public RNA-seq datasets against the Blank.hap1 assembly with only the best match retained. In brief, the raw reads were first processed to remove adaptor bases and low-quality sequences by Trimmomatic (https://github.com/timflutre/trimmomatic), and subsequently aligned to the reference using Subread (https://github.com/ShiLab-Bioinformatics/subread). Then, the read counts were estimated by featureCounts embedded in Subread and finally normalized to fragments per kilobase of transcripts per million mapped fragments. Specifically, these RNA-seq datasets were sequenced from male leaves, male flowers, male anther, female flowers, and fruits in three transcriptomic studies (Table S12).

Vector construction and plant transformation

Firstly, the full-length cDNA sequence of *AerYFT*, which has the accession number Aerbkv1a12g170990 in the KPGD database (Li et al., 2025), was cloned using reverse transcriptase-polymerase chain reaction (RT-PCR) and verified by Sanger sequencing. Subsequently, the coding region of *AerYFT* was inserted into the pBI121 at the *Xba*I and *Xho*I restriction sites. Then, the constructed pBI121-35S-*AerYFT* vector was introduced into the *Agrobacterium* GV3101. Finally, the *Agrobacterium*-mediated stable transformation of Arabidopsis was performed according to the floral dipping method (Clough & Bent, 1998). The homozygous lines of T2 generation were used for phenotypic observation.

Protein extraction and immunoblot analysis

Proteins in the leaves of transgenic Arabidopsis plants were extracted and isolated according to the procedure described previously (Huang et al., 2013). Firstly, protein extraction was boiled in 5× SDS loading buffer for 5 min and then resolved by SDS-PAGE. After transferring to polyvinylidene fluoride membranes, the boiled samples were blocked in blocking buffer (1× TTBS with 5% dried non-fat milk) for 2 h at room temperature. Subsequently, the blocked membranes were incubated with anti-HA-HRP (Roche, Basel, Basel-Stadt, Switzerland) and anti-HA (Sigma-Aldrich, Saint Louis, MO, USA) for another 1–2 h, respectively. Then, these membranes were washed with 1× TTBS buffer for 10 min, which required three times repetition. Finally, they were incubated with the appropriate secondary antibody for another 1 h in blocking buffer.

Visualization of statistics data

Generally, we used the R language to analyze and present our statistical results. In particular, the 'barplot' package was used to display histograms, the 'ggplots' package was used to display pie charts, scatter charts, and violin plots, and the 'ggcorrplot' package was used to display heatmaps of sequence similarity.

ACCESSION NUMBERS

All the gene and protein sequences of *FT* homologs can be found in the KPGD database (Li et al., 2025) under their respective accession numbers.

ACKNOWLEDGMENTS

We extend our appreciation to colleagues who documented the sexual dimorphism in kiwifruit flowering time through field observations across multiple populations. This work was supported by the National Natural Science Foundation of China (32472680 and U23A20204), Anhui Provincial Natural Science Foundation (2308085MC69), Key Scientific Research Foundation of the Education Department of Province Anhui (2024AH050452) and High-level Talent Funds of Anhui Agricultural University (rc322216 and rc322302).

AUTHOR CONTRIBUTIONS

JY, XY, SW, and YL conceived this project. JY, LX, and ZC analyzed the data. LX, TM, LW, and BL conducted the experiments. YL provided the hybrid population for phenotypic observation. JY, XY, and SW wrote the first manuscript. YL, EV-G, and ACA edited the manuscript. AZ produced the statistical charts in the manuscript. All authors revised and approved the final manuscript.

CONFLICT OF INTEREST

The authors declare no competing interests.

DATA AVAILABILITY STATEMENT

The data that support the findings of this study are available in the Supporting Information of this article.

SUPPORTING INFORMATION

Additional Supporting Information may be found in the online version of this article.

Figure S1. Comparative transcriptomic analysis of different kiwifruit tissues between males and females.

Figure S2. Schematic representation of the custom SynPanScan pipeline.

Table S1. Summary statistics of the 10 kiwifruit genome assemblies.

Table S2. Matrix of 52 775 non-redundant pan-gene orthogroups.

Table S3. Proportion of genes in different orthogroups from each genome assembly.

Table S4. Simulation of the pan-gene size with 500 replicates.

Table S5. The representative gene of each pan-gene orthogroup as well as its sequence characterize and functional annotation.

Table S6. The selected gene pairs of each pan-gene orthogroup used to compute *Ka*/*Ks* values.

Table S7. The enriched GO terms for the core genes in the constructed pan-genome of kiwifruit.

Table S8. The enriched GO terms for the dispensable genes in the constructed pan-genome of kiwifruit.

Table S9. The identification of syntenic gene sets with sex-differentiated occurrence.

Table S10. The genomic location of syntenic gene sets with sex-differentiated occurrence.

Table S11. The calculated values of sequence similarity, synonymous substitution (*Ks*) and non-synonymous substitution (*Ka*).

REFERENCES

Abdulla, M.F., **Mostafa, K.** & **Kavas, M.** (2024) CRISPR/Cas9-mediated mutagenesis of *FT*/*TFL1* in petunia improves plant architecture and early flowering. *Plant Molecular Biology*, **114**, 69.

Akagi, T., **Henry, I.M.**, **Ohtani, H.**, **Morimoto, T.**, **Beppu, K.**, **Kataoka, I.** ***et al.*** (2018) A Y-encoded suppressor of feminization arose via lineage-specific

duplication of a cytokinin response regulator in kiwifruit. *Plant Cell*, **30**, 780–795.

Akagi, T., **Pilkington, S.M.**, **Varkonyi-Gasic, E.**, **Henry, I.M.**, **Sugano, S.S.**, **Sonoda, M.** ***et al.*** (2019) Two Y-chromosome-encoded genes determine sex in kiwifruit. *Nature Plants*, **5**, 801–809.

Akagi, T., **Varkonyi-Gasic, E.**, **Shirasawa, K.**, **Catanach, A.**, **Henry, I.M.**, **Mertten, D.** ***et al.*** (2023) Recurrent neo-sex chromosome evolution in kiwifruit. *Nature Plants*, **9**, 393–402.

Barrett, S.C. & **Hough, J.** (2013) Sexual dimorphism in flowering plants. *Journal of Experimental Botany*, **64**, 67–82.

Blackman, B.K., **Strasburg, J.L.**, **Raduski, A.R.**, **Michaels, S.D.** & **Rieseberg, L.H.** (2010) The role of recently derived *FT* paralogs in sunflower domestication. *Current Biology*, **20**, 629–635.

Brown, G.R., **Laland, K.N.** & **Mulder, M.B.** (2009) Bateman's principles and human sex roles. *Trends in Ecology & Evolution*, **24**, 297–304.

Buchfink, B., **Reuter, K.** & **Drost, H.G.** (2021) Sensitive protein alignments at tree-of-life scale using DIAMOND. *Nature Methods*, **18**, 366–368.

Cheng, C.H., **Seal, A.G.**, **Murphy, S.J.** & **Lowe, R.G.** (2006) Variability and inheritance of flowering time and duration in *Actinidia chinensis* (kiwifruit). *Euphytica*, **147**, 395–402.

Clough, S.J. & **Bent, A.F.** (1998) Floral dip: a simplified method for *Agrobacterium*-mediated transformation of *Arabidopsis thaliana*. *The Plant Journal*, **16**, 735–743.

Delph, L.F., **Brown, K.E.**, **Ríos, L.D.** & **Kelly, J.K.** (2022) Sex-specific natural selection on SNPs in *Silene latifolia*. *Evolution Letters*, **6**, 308–318.

Emms, D.M. & **Kelly, S.** (2019) OrthoFinder: phylogenetic orthology inference for comparative genomics. *Genome Biology*, **20**, 238.

Ferguson, A.R. (1991) Kiwifruit (*Actinidia*). *Acta Horticulturae*, **290**, 603–656.

Han, X., **Zhang, Y.**, **Zhang, Q.**, **Ma, N.**, **Liu, X.**, **Tao, W.** ***et al.*** (2023) Two haplotype-resolved, gap-free genome assemblies for *Actinidia latifolia* and *Actinidia chinensis* shed light on the regulatory mechanisms of vitamin C and sucrose metabolism in kiwifruit. *Molecular Plant*, **16**, 452–470.

Huang, S., **Ding, J.**, **Deng, D.**, **Tang, W.**, **Sun, H.**, **Liu, D.** ***et al.*** (2013) Draft genome of the kiwifruit *Actinidia chinensis*. *Nature Communications*, **4**, 2640.

Jaillon, O., **Aury, J.M.**, **Noel, B.**, **Policriti, A.**, **Clepet, C.**, **Casagrande, A.** ***et al.*** (2007) The grapevine genome sequence suggests ancestral hexaploidization in major angiosperm phyla. *Nature*, **449**, 463–467.

Janzen, D.H. (1977) A note on optimal mate selection by plants. *The American Naturalist*, **111**, 365–371.

Jiang, X.D., **Zhong, M.C.**, **Dong, X.**, **Li, S.-B.** & **Hu, J.-Y.** (2022) Rosoideae-specific duplication and functional diversification of *FT-like* genes in Rosaceae. *Horticulture Research*, **9**, uhac059.

Jordan, C.Y. & **Charlesworth, D.** (2012) The potential for sexually antagonistic polymorphism in different genome regions. *Evolution*, **66**, 505–516.

Kaufmann, P., **Howie, J.M.** & **Immonen, E.** (2023) Sexually antagonistic selection maintains genetic variance when sexual dimorphism evolves. *Proceedings. Biological sciences*, **290**, 20222484.

Kaufmann, P., **Wolak, M.E.**, **Husby, A.** & **Immonen, E.** (2021) Rapid evolution of sexual size dimorphism facilitated by Y-linked genetic variance. *Nature Ecology & Evolution*, **5**, 1394–1402.

Kong, X., **Zhang, Y.**, **Wang, Z.**, **Bao, S.**, **Feng, Y.**, **Wang, J.** ***et al.*** (2023) Two-step model of paleohexaploidy, ancestral genome reshuffling and plasticity of heat shock response in Asteraceae. *Horticulture Research*, **10**, uhad073.

Larkin, M.A., **Blackshields, G.**, **Brown, N.P.**, **Chenna, R.**, **McGettigan, P.A.**, **McWilliam, H.** ***et al.*** (2007) Clustal W and Clustal X version 2.0. *Bioinformatics*, **23**, 2947–2948.

Li, B., **Li, X.**, **Wang, Y.**, **Liu, X.**, **Li, K.**, **Li, R.** ***et al.*** (2025) KPGD: a kiwifruit pan-genome database for comprehensive mining of genetic diversity in the genus *Actinidia*. *Plant Communications*, **13**, 101373.

Li, J., **Li, X.** & **Soejarto, D.** (2007) Actinidiaceae. In: Wu, Z., Raven, P. & Hong, D. (Eds.) *Flora of China*, Vol. **12**. Beijing, China: Science Press, pp. 334–362.

Liu, Y., **Zhou, Y.**, **Cheng, F.**, **Zhou, R.**, **Yang, Y.**, **Wang, Y.** ***et al.*** (2024) Chromosome-level genome of putative autohexaploid *Actinidia deliciosa* provides insights into polyploidisation and evolution. *The Plant Journal*, **118**, 73–89.

Madeira, F., **Madhusoodanan, N.**, **Lee, J.**, **Eusebi, A.**, **Niewielska, A.**, **Tivey, A.R.N.** ***et al.*** (2024) The EMBL-EBI job dispatcher sequence analysis tools framework in 2024. *Nucleic Acids Research*, **52**, W521–W525.

Ming, R., **Bendahmane, A.** & **Renner, S.S.** (2011) Sex chromosomes in land plants. *Annual Review of Plant Biology*, **62**, 485–514.

Moss, S.M.A., **Wang, T.**, **Voogd, C.**, **Brian, L.A.**, **Wu, R.**, **Hellens, R.P.** ***et al.*** (2018) *AcFT* promotes kiwifruit *in vitro* flowering when overexpressed and Arabidopsis flowering when expressed in the vasculature under its own promoter. *Plant Direct*, **2**, e00068.

Mota, L., **Torices, R.** & **Loureiro, J.** (2016) The evolution of haploid chromosome numbers in the sunflower family. *Genome Biology and Evolution*, **8**, 3516–3528.

Navarro, C., **Abelenda, J.A.**, **Cruz-Oró, E.**, **Cuéllar, C.A.**, **Tamaki, S.**, **Silva, J.** ***et al.*** (2011) Control of flowering and storage organ formation in potato by *FLOWERING LOCUS T*. *Nature*, **478**, 119–122.

Pennell, T.M., **de Haas, F.J.**, **Morrow, E.H.** & **van Doorn, G.** (2016) Contrasting effects of intralocus sexual conflict on sexually antagonistic coevolution. *Proceedings of the National Academy of Sciences of the United States of America*, **113**, E978–E986.

Reyes-Chin-Wo, S., **Wang, Z.**, **Yang, X.**, **Kozik, A.**, **Arikit, S.**, **Song, C.** ***et al.*** (2017) Genome assembly with *in vitro* proximity ligation data and whole-genome triplication in lettuce. *Nature Communications*, **8**, 14953.

Song, G.Q., **Walworth, A.**, **Lin, T.**, **Chen, Q.**, **Han, X.**, **Irina Zaharia, L.** ***et al.*** (2019) *VcFT*-induced mobile florigenic signals in transgenic and transgrafted blueberries. *Horticulture Research*, **6**, 105.

Spencer, S.C. & **Rieseberg, L.H.** (1995) The importance of flowering time and flower number in the relative fitness of males and hermaphrodites in *Datisca glomerata* (Datiscaceae). *Plant Species Biology*, **10**, 65–69.

Sun, J., **Wang, H.**, **Ren, L.**, **Chen, S.**, **Chen, F.** & **Jiang, J.** (2017) *CmFTL2* is involved in the photoperiod- and sucrose-mediated control of flowering time in chrysanthemum. *Horticulture Research*, **4**, 17001.

Svensson, E.I., **Goedert, D.**, **Gómez-Llano, M.A.**, **Spagopoulou, F.**, **Nava-Bolaños, A.** & **Booksmythe, I.** (2018) Sex differences in local adaptation: what can we learn from reciprocal transplant experiments? *Philosophical Transactions of the Royal Society, B: Biological Sciences*, **373**, 20170420.

Tamura, K., **Stecher, G.** & **Kumar, S.** (2021) MEGA11: molecular evolutionary genetics analysis version 11. *Molecular Biology and Evolution*, **38**, 3022–3027.

Testolin, R. (1991) Male density and arrangement in kiwifruit orchards. *Acta Horticulturae*, **48**, 41–50.

Varkonyi-Gasic, E., **Moss, S.M.A.**, **Voogd, C.**, **Wang, T.**, **Putterill, J.** & **Hellens, R.P.** (2013) Homologs of *FT*, *CEN* and *FD* respond to developmental and environmental signals affecting growth and flowering in the perennial vine kiwifruit. *New Phytologist*, **198**, 732–746.

Varkonyi-Gasic, E., **Wang, T.**, **Cooney, J.**, **Jeon, S.**, **Voogd, C.**, **Douglas, M.J.** ***et al.*** (2021) *Shy girl*, a kiwifruit suppressor of feminization, restricts gynoecium development via regulation of cytokinin metabolism and signalling. *The New Phytologist*, **230**, 1461–1475.

Voogd, C., **Brian, L.A.**, **Wang, T.**, **Allan, A.C.** & **Varkonyi-Gasic, E.** (2017) Three *FT* and multiple *CEN* and *BFT* genes regulate maturity, flowering, and vegetative phenology in kiwifruit. *Journal of Experimental Botany*, **68**, 1539–1553.

Wan, M., **Zhao, D.**, **Lin, S.**, **Wang, P.**, **Liang, B.**, **Jin, Q.** ***et al.*** (2024) Allelic variation of *BnaFTA2* and *BnaFTC6* is associated with flowering time and seasonal crop type in rapeseed (*Brassica napus* L.). *Plant, Cell & Environment*, **48**, 852–865.

Wang, L., **Yang, N.**, **Chen, M.**, **Wang, L.-L.**, **Yang, N.-C.**, **Chen, M.-Y.** ***et al.*** (2021) Polyploidization and sexual dimorphism of floral traits in a subdioecious population of *Dasiphora glabra*. *Journal of Plant Ecology*, **14**, 229–240.

Wang, Y., **Dong, M.**, **Wu, Y.**, **Zhang, F.**, **Ren, W.**, **Lin, Y.** ***et al.*** (2023) Telomere-to-telomere and haplotype-resolved genome of the kiwifruit *Actinidia eriantha*. *Molecular Horticulture*, **3**, 4.

Wang, Y., **Li, P.**, **Zhu, Y.**, **Zhang, F.**, **Zhang, S.**, **He, Y.** ***et al.*** (2024) Graph-based pangenome of *Actinidia chinensis* reveals structural variations mediating fruit degreening. *Advanced Science*, **11**, e2400322.

Wang, Y., **Tang, H.**, **Debarry, J.D.**, **Tan, X.**, **Li, J.**, **Wang, X.** ***et al.*** (2012) MCScanX: a toolkit for detection and evolutionary analysis of gene synteny and collinearity. *Nucleic Acids Research*, **40**, e49.

Wickland, D.P. & **Hanzawa, Y.** (2015) The *FLOWERING LOCUS T/TERMINAL FLOWER 1* gene family: functional evolution and molecular mechanisms. *Molecular Plant*, **8**, 983–997.

Williams, T.M. & **Carroll, S.B.** (2009) Genetic and molecular insights into the development and evolution of sexual dimorphism. *Nature Reviews. Genetics*, **10**, 797–804.

Wu, D., **Xie, L.**, **Sun, Y.**, **Huang, Y.**, **Jia, L.**, **Dong, C.** ***et al.*** (2023) A syntelog-based pan-genome provides insights into rice domestication and de-domestication. *Genome Biology*, **24**, 179.

Yang, Z. (2007) PAML 4: phylogenetic analysis by maximum likelihood. *Molecular Biology and Evolution*, **24**, 1586–1591.

Yang, Z., **Gu, S.**, **Wang, X.**, **Li, W.**, **Tang, Z.** & **Xu, C.** (2008) Molecular evolution of the *CPP-like* gene family in plants: insights from comparative genomics of Arabidopsis and rice. *Journal of Molecular Evolution*, **67**, 266–277.

Yang, Z., **Qian, S.**, **Scheid, R.N.**, **Lu, L.**, **Chen, X.**, **Liu, R.** ***et al.*** (2018) EBS is a bivalent histone reader that regulates floral phase transition in Arabidopsis. *Nature Genetics*, **50**, 1247–1253.

Yao, X., **Wang, S.**, **Wang, Z.**, **Li, D.**, **Jiang, Q.**, **Zhang, Q.** ***et al.*** (2022) The genome sequencing and comparative analysis of a wild kiwifruit *Actinidia eriantha*. *Molecular Horticulture*, **2**, 13.

Yu, W., **Wang, X.**, **Wang, H.**, **Wang, W.**, **Cheng, H.**, **Mei, D.** ***et al.*** (2025) Optimization and application of genome prediction model in rapeseed: flowering time, yield components, and oil content as examples. *Horticulture Research*, **12**, uhaf115.

Yu, X., **Qin, M.**, **Qu, M.**, **Jiang, Q.**, **Guo, S.**, **Chen, Z.** ***et al.*** (2023) Genomic analyses reveal dead-end hybridization between two deeply divergent kiwifruit species rather than homoploid hybrid speciation. *The Plant Journal*, **115**, 1528–1543.

Yue, J., **Chen, Q.**, **Wang, Y.**, **Zhang, L.**, **Ye, C.**, **Wang, X.** ***et al.*** (2023) Telomere-to-telomere and gap-free reference genome assembly of the kiwifruit *Actinidia chinensis*. *Horticulture Research*, **10**, uhac264.

Yue, J., **Chen, Q.**, **Zhang, S.**, **Lin, Y.**, **Ren, W.**, **Li, B.** ***et al.*** (2024) Origin and evolution of the kiwifruit Y chromosome. *Plant Biotechnology Journal*, **22**, 287–289.

Zheng, R., **Meng, X.**, **Hu, Q.**, **Yang, B.**, **Cui, G.**, **Li, Y.** ***et al.*** (2023) *OsFTL12*, a member of *FT-like* family, modulates the heading date and plant architecture by florigen repression complex in rice. *Plant Biotechnology Journal*, **21**, 1343–1360.

Zheng, J. & **Xia, R.** (2022) Flower development and sex determination in horticultural crops. *Fruit Research*, **2**, 9.